Nonlinear Processes in Geophysics

Physical simulation of resonant wave run-up on a beach

A. Ezersky[1], N. Abcha[1], and E. Pelinovsky[2,3,4]

[1]CNRS, UMR6143 – Morphodynamique Continentale et Côtière (M2C), Université Caen Basse, Normandie,
24 rue des Tilleuls, 14000 Caen, France
[2]Institute of Applied Physics, 46, Ul'janov St., Nizhny Novgorod 603950, Russia
[3]Nizhny Novgorod State Technical University, Nizhny Novgorod, Russia
[4]National Research University – Higher School of Economics, Nizhny Novgorod, Russia

Correspondence to: E. Pelinovsky (pelinovsky@hydro.appl.sci-nnov.ru)

Abstract. Nonlinear wave run-up on the beach caused by a harmonic wave maker located at some distance from the shore line is studied experimentally. It is revealed that under certain wave excitation frequencies, a significant increase in run-up amplification is observed. It is found that this amplification is due to the excitation of resonant mode in the region between the shoreline and wave maker. Frequency and magnitude of the maximum amplification are in good correlation with the numerical calculation results represented in the paper (Stefanakis et al., 2011). These effects are very important for understanding the nature of rogue waves in the coastal zone.

1 Introduction

Recent huge tsunamis demonstrate nonlinear behaviour on the coast leading to strong impact. It was also revealed recently that the number of abnormally large and suddenly appearing waves (rogue waves) observed in the coastal zone is sufficiently larger than Gaussian statistics predicts (Nikolkina and Didenkulova, 2011, 2012). Analysis of tsunami records showed that reflections due to bottom topography may result in the appearance of resonant mode in the coastal zone, see for instance Neetu et al. (2011). The study of the coastal rogue waves is based on the nonlinear theory of shallow water (Kharif et al., 2009; Didenkulova and Pelinovsky, 2011; Slunyaev et al., 2011). To characterize the impact of waves on coastal infrastructure, the systematic study of run-up process is undertaken, and a lot of papers summarizing the progress in the analytical solutions of the nonlinear shallow-water theory have been published by now (see

for instance Carrier and Greenspan, 1958; Pelinovsky, 1982; Synolakis, 1987; Pelinovsky and Mazova, 1992; Carrier et al., 2003; Kânoğlu and Synolakis, 2006; Didenkulova et al., 2007; Madsen and Fuhrman, 2008; Kajiura, 1977). Recently, Stefanakis et al. (2011), on the basis of numerical simulations of the nonlinear shallow-water equations, pointed out the existence of resonance effects in the process of the long wave run-up. It should be noted that such resonance effects were predicted in Antuono and Brocchini (2010) in the framework of linear theory.

The main result of Stefanakis et al. (2011) is that at a certain frequency of the waves there exists a significant increase in the run-up amplitude. According to calculations, the maximal run-up height can be 50 times greater than the free surface oscillation amplitude used as the boundary condition in the numerical calculations. It should be emphasized that the estimations presented in the different papers cited above provide us an order of maximal run-up height much less than in Stefanakis et al. (2011). It was established in Stefanakis et al. (2011) that the wave period for which maximal run-up amplification is observed depends on the slope of the bottom and the depth of water in the place where the waves are excited. This period is much larger than the "natural period" – time needed for perturbations to run from the point of excitation to the shoreline and return back. Results obtained in Stefanakis et al. (2011) pose a lot of questions. That is why in order to investigate the physical mechanisms of run-up amplification, needed to explain the coastal extreme rouge waves, we carried out a physical simulation of this process in the hydrodynamic channel with an inclined bottom. The simulation is carried out in such a way that its results can be

used for comparison with numerical calculations presented in Stefanakis et al. (2011).

Before the presentation of experimental results, we give briefly some theoretical estimates. The long wave run-up on a plane beach is described by the nonlinear shallow-water equations:

$$\frac{\partial u}{\partial t} + u\frac{\partial u}{\partial x} + g\frac{\partial \eta}{\partial x} = 0 \text{ and}$$
$$\frac{\partial \eta}{\partial t} + \frac{\partial}{\partial x}\left(u\left(h+\eta\right)\right) = 0 \qquad (1)$$

where u is the depth-averaged velocity, $h = h(x)$ is the unperturbed water depth, $\eta = \eta(x,t)$ is the free surface displacement, and g is the acceleration of gravity. For linear variation of water depth, $h = x\theta$ (θ is the tangent of bottom slope angle, x is horizontal coordinate), solutions of these equations may be found using the hodograph transformation (details can be found in papers Carrier and Greenspan, 1958; Pelinovsky, 1982; Synolakis, 1987; Pelinovsky and Mazova, 1992; Carrier et al., 2003; Kânoğlu and Synolakis, 2006; Didenkulova et al., 2007; Madsen and Fuhrman, 2008; Kajiura, 1977). For instance, if the incident wave far from the shore is a monochromatic wave of frequency ω, the solution is presented in the following form:

$$\eta = \frac{1}{2g}\left(\frac{\partial\varphi}{\partial\lambda}-u^2\right), \quad u = \frac{1}{\sigma}\frac{\partial\varphi}{\partial\sigma},$$
$$x = \frac{1}{2g\theta}\left(\frac{\partial\varphi}{\partial\lambda}-u^2-\frac{\sigma^2}{2}\right), \quad t = \frac{\lambda-u}{g\theta}, \text{ and}$$
$$\varphi(\sigma,\lambda) = \frac{2g\theta^2}{\omega}RJ_0\left(\omega\lambda/\theta g\right)\sin\left(\omega\lambda/\theta g\right) \qquad (2)$$

where $\varphi(\sigma,\lambda)$ is an auxiliary function, $\sigma = 2[g(h+\eta)]^{1/2}$, and J_0 is the Bessel function of zero order. Generally speaking, wave field in the vicinity of the shoreline ($x = 0$) is not monochromatic, but if the nonlinear effects are ignored, the solution (Eq. 2) is written in the following form:

$$\eta(x,t) = RJ_0\left(\sqrt{4\omega^2x/g\theta}\right)\cos\left(\omega t\right). \qquad (3)$$

It is a standing wave with knots coinciding with zeros of the Bessel function. The constant R plays the role of the amplitude of the water oscillation on "unmoved" shore ($x = 0$). As it can be rigorously shown from Eq. (2), R is the maximal run-up amplitude of the wave on the coast (moving shoreline) (Pelinovsky and Mazova, 1992). Far from the shoreline the wave is always linear because its amplitude is much less than water depth. Using asymptotics of the Bessel functions for large values of arguments, we can select the incident wave with amplitude A at the distance L from the shoreline and obtain the amplification ratio in the following form (Pelinovsky, 1982; Pelinovsky and Mazova, 1992; Madsen and Fuhrman, 2008):

$$R/A = 2\sqrt{\pi}\left(h_0\omega^2/g\theta^2\right)^{1/4} = 2\pi\sqrt{2L/\lambda_0}, \qquad (4)$$

where λ_0 is the wavelength on the isobath h_0 located on distance L from the shore. It is important to point out that the asymptotic (Eq. 4) is valid for large values of L/λ_0 and represents nonlinear amplification ration obtained directly from Eq. (2). In the case of small values of L/λ_0, correct selection of incident and reflected waves is possible if the beach of length L is matched with flat bottom. In this case the amplification ratio is given by Pelinovsky (1982), Pelinovsky and Mazova (1992), Madsen and Fuhrman (2008), and Keller and Keller (1964):

$$R/A = 2/\sqrt{J_0^2\left(4\pi L/\lambda_0\right)+J_1^2\left(4\pi L/\lambda_0\right)}. \qquad (5)$$

Comparison of Eqs. (4) and (5) is given in Fig. 1. As it can be seen, the resonance effects are very small because the "resonator" ($0 < x < L$) is open from one boundary. For tsunami application, the characteristics of the incident wave very often are unknown. Meanwhile, a lot of buoys are now installed along the coasts (tide-gauge stations and DART buoys), and tsunami records on such buoys can be considered as input for solving the run-up problem. In the simplified geometry of a plane beach, the buoy measures the standing wave (Eqs. 2 or 3), and in the case of small wave amplitude, free surface oscillations are described by:

$$\eta(L,t) = a\cos\left(\omega t\right), \text{ and } \quad a = RJ_0\left(\sqrt{4\omega^2 L/g\theta}\right). \qquad (6)$$

The amplification factor computed for the tsunami wave propagated from the buoy to the coast,

$$C = R/a = J_0^{-1}\left(\sqrt{4\omega^2 L/g\theta}\right), \qquad (7)$$

has evident resonant properties and can be very large. Such big values of local amplification factors have been discovered in a recent paper (Stefanakis et al., 2011) where the result was obtained by numerical computation. In fact, it is not the resonance caused by a particular frequency of incoming wave but instead a ratio between the run-up and the wave amplitude measured at a particular distance from the coastline. This amplification of run-up ratio can be very important for prediction of tsunami behaviour based on data of the nearest buoy. Following Stefanakis et al. (2011), we call amplification of run-up ratio at particular frequencies as resonance. Analytical and numerical results described above are examined below in physical experiment.

Experiments were performed in a long hydrodynamic flume of 0.5 m width. The flume is equipped with a wave maker controlled by computer. To simulate an inclined bottom, a PVC plate with thickness of 1 cm is used. The plate is placed at different angles relative to the horizontal bottom of the flume in the vicinity of the wave maker (see Fig. 2). Three series of experiments have been performed for water depth h near the wave maker and length L, ($h_0 = 0.245$ m, $L = 145.8$ m, $\theta = 0.168$) ($h_0 = 0,26$ m,
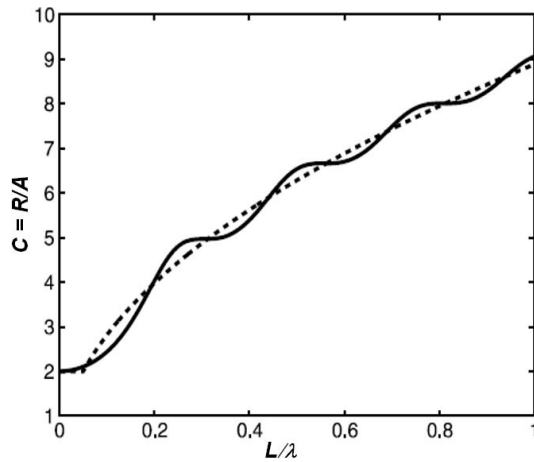
Fig. 1. Amplification run-up ratio: dashed line corresponds to the constant beach slope Eq. (4); solid line obtained for inclined beach matched with horizontal bottom Eq. (5).

Fig. 2. Schema of experiment: resistive probes (P1, P2), high-speed video camera (2), wave maker (3), inclined bottom (4).

$L = 135$ m, $\theta = 0.192$) and ($h_0 = 0.32$ m, $L = 121.5$ m, $\theta = 0.263$). Two resistive probes (P1, P2, see Fig. 2) are used to measure a displacement of water surface. The first of them, probe P1, is placed at a fixed distance of 1 cm from the wave maker. The position of a mobile one, P2, is changed using a coordinate system. Probes allow us to investigate the amplitude of free surface oscillations and phase of oscillation (probe P1 is used as a "clock") along the flume. Run-up height is determined by processing a movie that is shot by a high-speed camera mounted as shown in Fig. 2. The wave maker allows us to excite a harmonic wave of a given frequency and it works in two regimes. The first regime allows controlling the amplitude of wave maker displacement, the second one allows controlling the amplitude of force applied to the wave maker. In both regimes it is not possible to control free surface displacement, as was done in the numerical experiment. That is why to study the run-up amplification, simultaneous measurements of the amplitude of free surface displacement near the wave maker and maximal run-up are carried out for different frequencies of excitation.

The force control regime was chosen for all experiments. The frequency dependence of the amplitude of free surface displacement near the wave maker (a), maximal run-up (R) and coefficient of run-up amplification are shown in Fig. 3 for the slope of the bottom $\theta = \tan(\alpha) = 0.263$. The amplitude of force applied to the wave maker was the same for all frequencies. The amplitude of free surface displacement has peaks at frequencies $f_1 = 0.44$ Hz and $f_2 = 0.78$ Hz. They are the resonant frequencies of the system. The maximal run-up does not have sharp peaks, only a small increase of R in the vicinity of f_1 and f_2 is observed (Fig. 3b). The coefficient of run-up amplification (Fig. 3c) increases very sharply in the vicinity of $f_3 = 0.28$ Hz and $f_4 = 0.64$ Hz. It is evident that maximal amplification of run-up is observed for frequencies corresponding to the minimal amplitude a. In
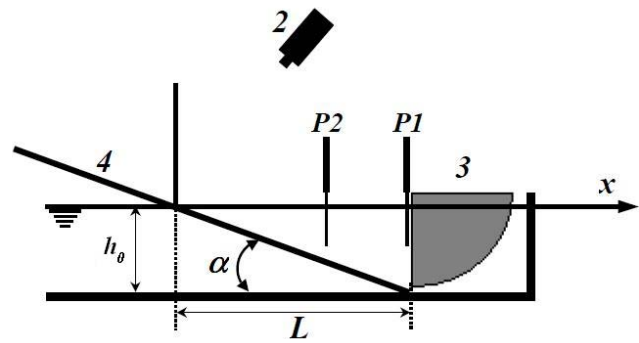
the vicinity of the wave maker, the free surface amplitude is sufficiently small and the signal is very noisy. That is why the coefficient of run-up amplification requires rather delicate measurements of free surface displacement: a band-pass filter was used to measure the amplitude of the harmonic corresponding to wave maker forcing.

It is important to note that the frequency and the coefficient of maximal amplification do not depend on the method of wave excitation. Results presented in Fig. 3 were obtained for the force-controlled regime of the wave maker; the same results for coefficient of run-up amplification were obtained for the displacement controlled regime. It should be noted that if the amplitude of force applied to the wave maker increases, the coefficient of run-up amplification has small changes up to the appearance of wave breaking near the coastline.

Using movie recorded by a high-speed camera, we estimate the so-called wave-breaking number "Br" (Denissenko et al., 2011): $\text{Br} = \frac{V^2}{gR}$, where V is velocity of fluid particles at $x = 0$. Under our experimental conditions, this number is small enough: $\text{Br} < 0.2$.
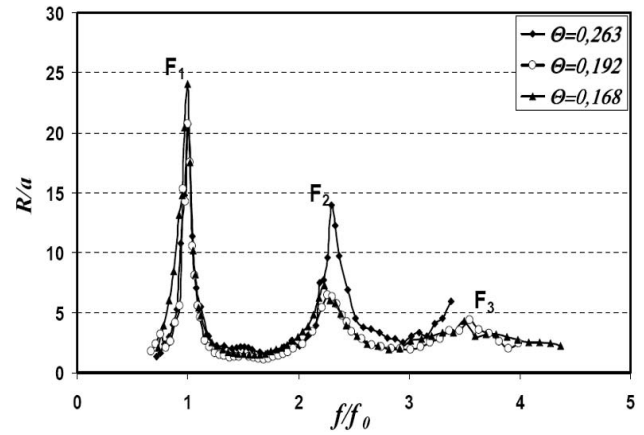
Amplification coefficient C was investigated for three bottom inclinations. Frequencies of maximal amplification depend on angle α. To compare results obtained for different angles α, the non-dimensional frequency (F) was introduced: $F = f/f_0$, $f_0 = K^{-1}(g/h_0)^{1/2}\theta$, and $K = 5.23$. Results are presented in Fig. 4. Non-dimensional frequencies of maximal run-up amplification $F_1 = 1$ for different angles α coincide very precisely. The coefficient of maximal amplification, corresponding to the frequency $F_1 = 1$, is approximately the same for different inclinations: $C \sim 20$–25. The second peak of run-up amplification coefficient is observed for frequency $F_2 = (2.2$–$2.3) F_1$. Non-dimensional frequency F_2 slightly depends on bottom slope; a small peak is observed also for frequency $F_3 \sim 3.5 F_1$.

It should be noted that in our experimental conditions, run-up without wave breaking is observed for small frequencies of wave excitation of $F < 2$, while for higher excitation frequencies of $F > 2$ near $x = 0$, the surface wave becomes strongly nonlinear and run-up occurs after the wave breaking.
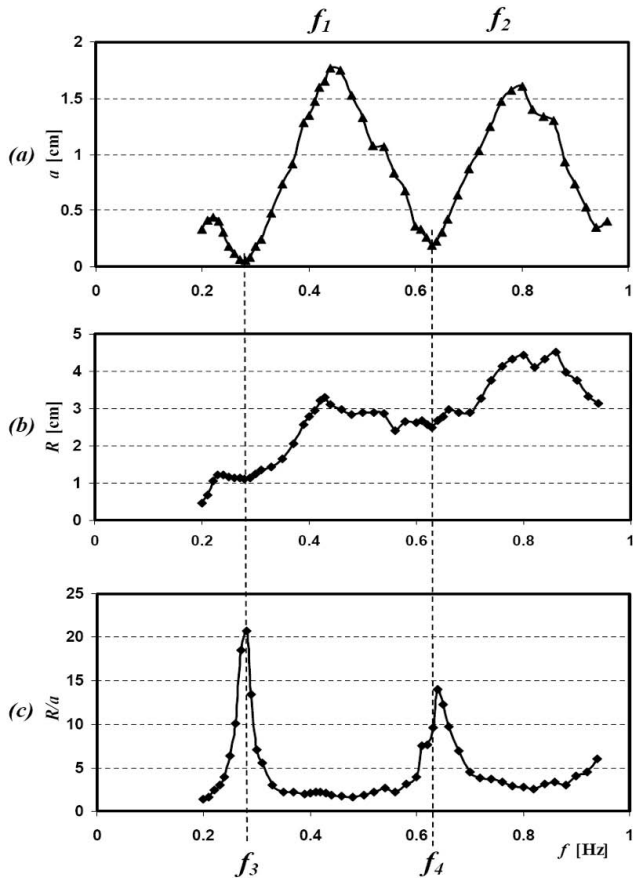
Fig. 3. Frequency dependence of amplitude on free surface displacement (resonance curve) **(a)**, maximal run-up **(b)** and amplification of run-up (ratio of the maximal run-up and the amplitude of surface wave) **(c)** for slope $\tan\alpha = 0.263$.

**Fig. 4.** Dependence of run-up amplification on normalized frequency for different bottom slopes.

The wave breaking does not prevent precise determination of maximal run-up position. Excepting high frequencies of $F > 3$, the wave front on a sloping beach was one dimensional, and maximal run-up did not depend on coordinates along the direction perpendicular to axis x. To study frequency dependence of run-up amplification more precisely, the spatial structures of the free surface oscillations occurring at frequencies corresponding to the resonant frequencies of the system ($f_1 = 0.34$ Hz, $f_2 = 0.58$ Hz) and at frequencies of maximum run-up amplification ($f_3 = 0.205$ Hz, $f_4 = 0.46$ Hz) have been investigated. The results are shown in Fig. 5 for bottom slope $\theta = 0.168$. Amplitude and phase of free surface displacement are shown by diamonds and circles. Experimental data are compared with the analytical solution (Eq. 3) for free surface displacement η. Theoretical curves obtained from Eq. (3) are shown in Fig. 5 by thick lines. The amplitude a and the phase ϕ of free surface harmonic oscillations are shown in Fig. 5. Because the Bessel function changes sign, amplitude is chosen as $a = |J_0|$, $\phi = 0$ if $J_0 > 0$ and $\phi = \pi$ if $J_0 < 0$. One can find in Fig. 5 that in the experiment the amplitude does not go to zero and

phase changes smoothly for all frequencies. Note that frequencies of maximal run-up amplification ($f_3 = 0.205$ Hz, $f_4 = 0.46$ Hz) correspond to spatial modes having minimal amplitudes near the wave maker; resonance frequencies ($f_1 = 0.34$ Hz, $f_2 = 0.58$ Hz) have maximum amplitudes of free surface displacement near the wave maker. It should be noted that according to the solution (Eq. 1), frequencies of maximal run-up amplification correspond to the spatial modes with boundary condition $\eta(L, t) = 0$, and resonant frequencies correspond to mode with boundary condition $\partial\eta(L, t)/\partial x = 0$. In other words, if one uses the linear solution (Eq. 1), the coefficient of run-up amplification in this approximation would be infinite: $a = 0$ at $x = L$. In the experiment, the amplitude is small, but finite. Comparison of curves presented in Fig. 5a,b,c,d shows that differences between the theoretical solution and experimental data increase with frequency of excitation. For example, these differences are much more significant for f_2 than for f_3.

Let us compare the experimental results with numerical simulations (Stefanakis et al., 2011). The numerical simulations on run-up were prepared for fixed amplitude of free surface displacement as a boundary condition at $x = L$. In the experiment, unlike the numerical calculations, it is not possible to generate waves with fixed amplitude at a definite coordinate. Instead it, the simultaneous measurements of the free surface displacement in the vicinity of wave maker and maximal run-up have been performed. In our experiment, the frequencies of maximal run-up amplification are very close to those that were obtained in the numerical calculation. We estimated the frequencies of the first peak as $f_3 = f_0 = K^{-1}(g/h_0)^{1/2}\theta$, $K = 5.23$; in Stefanakis et al. (2011) the coefficient is estimated as $K \sim 5.1$. The second peak f_4 in the experimental frequency dependence of run-up is more visible than in numerical simulation (Stefanakis et al., 2011). Authors Stefanakis et al. (2011) did not give any estimations of the second frequency peak, but if one uses
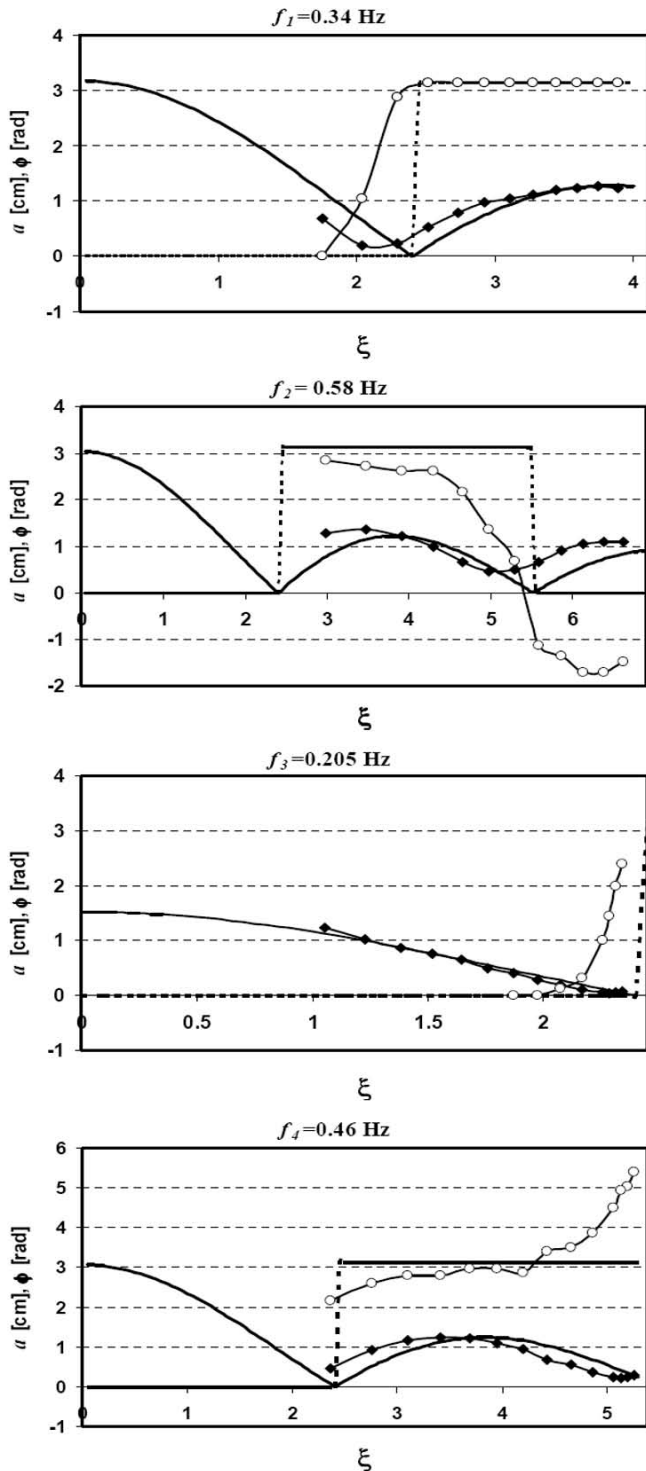
Fig. 5. Comparison of the experimental values of amplitude (diamonds) and phase (circles) with theoretical values of amplitude (thick solid lines) and phase (thick dashed lines) obtained from the Eq. (3), $\xi = \sqrt{4\omega^2 x / g\theta}$, $\theta = 0.168$; ends of horizontal axes correspond the positions of the wave-maker edge.

their data, it is possible to conclude that frequency of the second peak is 2.5–2.7 times more than frequency of the first one. In our experiments the frequency of the second peak exceeds the frequency of the first one 2.2–2.3 times. Experimental values of frequencies f_{3-4} practically coincide with frequencies of modes having nodes near the wave maker; numerical values (Stefanakis et al., 2011) exceed this frequency by 2.5 % for all bottom inclinations. The reason of such differences is not clear yet. Nonlinearity, wave dispersion, and viscous dissipation influence the frequency of these peaks, but simple estimations for linear waves in shallow water with zero viscosity provide values which are close to experimental data. Authors Stefanakis et al. (2011) do not mention any dissipation of energy and nonlinear parameter, which they use in numerical simulations. As for the coefficient of run-up amplification, the maximal value that was observed in the experiment is $C = 20$–25, whereas in Stefanakis et al. (2011) this value reaches $C = 50$–60. The difference is apparently due to viscous dissipation, which is essential in our experiments. In addition, capillary effects can also affect the run-up if the value of run-up R is comparable with the capillary length $R_{\text{cap}} = \sqrt{(2\gamma/\rho g)}$ (γ is coefficient of water surface tension, ρ is water density). This fact was mentioned in Denissenko et al. (2011). For our experiment, $R_{\text{cap}} = 3$ mm, for the most part the run-up measurements give us significantly higher values. Nevertheless, for the maximum amplification, the run-up is only 4 times more than the capillary length. Therefore, the decrease of coefficient C in comparison with the theoretical value may be partly due to the capillary effect.

2 Conclusions

On the basis of experiments, we can conclude that the value of amplification coefficients and frequencies at which run-up amplification maxima are observed correlate with results of numerical simulations. The most important conclusion is that the existence of an abnormally large increase of the coefficient C is due to resonator modes; this coefficient becomes very large because for its determination the amplitude at the mode node is taken as the amplitude of free surface displacement. This effect is very important for the prediction of tsunami run-up using the tide-gauge data. It is not sufficient to know the amplitude of free surface displacement in the near-shore zone; to provide the correct predictions of run-up, it is necessary to know if this value corresponds to the amplitude A of a propagating wave or to the amplitude a of a standing wave at a fixed point. Therefore, it is necessary to install several gauges in the coastal zone.

References

Antuono, M. and Brocchini, M.: Solving the nonlinear shallow-water equations in physical sense, J. Fluid Mech., 643, 207–232, 2010.

Carrier, G. F. and Greenspan, H. P.: Water waves of finite amplitude on a sloping beach, J. Fluid Mech., 4, 97–109, 1958.

Carrier, G. F., Wu, T. T., and Yeh, H.: Tsunami run-up and draw-down on a plane beach, J. Fluid Mech., 475, 79–99, 2003.

Denissenko, P., Didenkulova, I., Pelinovsky, E., and Pearson, J.: Influence of the nonlinearity on statistical characteristics of long wave runup, Nonlin. Processes Geophys., 18, 967–975, doi:10.5194/npg-18-967-2011, 2011.

Didenkulova, I. and Pelinovsky, E.: Rogue waves in nonlinear hyperbolic systems (shallow-water framework), Nonlinearity, 24, R1–R18, 2011.

Didenkulova, I., Pelinovsky, E., Soomere, T., and Zahibo, N.: Runup of nonlinear asymmetric waves on a plane beach, in: Tsunami and Nonlinear Waves, edited by: Kundu, A., 175–190, 2007.

Kajiura, K.: Local behavior of tsunamis, in: Waves on Water of Variable Depth, edited by: Provism D. and Radok, R., Lecture Notes in Physics, Vol. 64, Springer, Berlin, 72–79, 1977.

Kânoğlu, U. and Synolakis, C.: Initial value problem solution of nonlinear shallow-water equations, Phys. Rev. Lett., 97, 148501, doi:10.1103/PhysRevLett.97.148501, 2006.

Keller, J. B. and Keller, H. B.: ONR Research Report Contract No. NONR-3828(00), 1964.

Kharif, Ch., Pelinovsky, E., and Slunyaev, A.: Rogue waves in the ocean, Springer, Berlin, Heidelberg, New York, 2009.

Madsen, P. A. and Fuhrman, D. R.: Run-up of tsunamis and long waves in terms of surf-similarity, Coastal Eng., 55, 209–223, 2008.

Neetu, S., Suresh, I., Shankar, R., Nagarajan, B., Sharma, R., Shenoi, S. S. C., Unnikrishnan, A. S., and Sundar, D.: Trapped waves of the 27 November 1945 Makran tsunami: observations and numerical modelling, Nat. Hazards, 59, 1609–1618, 2011.

Nikolkina, I. and Didenkulova, I.: Rogue waves in 2006–2010, Nat. Hazards Earth Syst. Sci., 11, 2913–2924, doi:10.5194/nhess-11-2913-2011, 2011.

Nikolkina, I. and Didenkulova, I.: Catalogues of rogue waves reported in media in 2006–2010, Nat. Hazards, 61, 989–1006, 2012.

Pelinovsky, E.: Nonlinear dynamics of tsunami waves, Institute of Applied Physics, Nizhny Novgorod, 1982 (in Russian).

Pelinovsky, E. and Mazova, R.: Exact analytical solutions of nonlinear problems of tsunami wave run-up on slopes with different profiles, Nat. Hazards, 6, 227–249, 1992.

Slunyaev, A., Didenkulova, I., and Pelinovsky, E.: Rogue waters, Contemp. Phys., 52, 571–590, 2011.

Stefanakis, T. S., Dias, F., and Dutykh, D.: Local run-up amplification by resonant wave interaction, Phys. Rev. Lett., 107, 124502, doi:10.1103/PhysRevLett.107.124502, 2011.

Synolakis, C. E.: The runup of solitary waves, J. Fluid Mech., 185, 523–545, 1987.